Effect of Different Thermal Treatments on the Mechanical Performance of Poly(L-lactic acid) Based Eco-composites

T. Dobreva,[1] R. Benavente,[2] J. M. Pereña,[2] E. Pérez,[2] M. Avella,[3] M. García,[4] G. Bogoeva-Gaceva[5]

[1]*Central Laboratory of Physico-Chemical Mechanics, BAS, Sofia 1113, Bulgaria*
[2]*Department of Physical Chemistry, Instituto de Ciencia y Tecnología de Polímeros, CSIC, Juan de la Cierva 3, Madrid 28006, Spain*
[3]*Institute of Chemistry and Technology of Polymers, National Research Council, Pozzuoli (NA) 80078, Italy*
[4]*Materials and Sustainable Chemistry Department, Cidemco, Technological Research Centre, Azpeitia (Gipuzkoa) 20730, Spain*
[5]*Faculty of Technology and Metallurgy, University Sts. Cyril and Metodius, Skopje 1000, Republic of Macedonia*

Received 17 April 2009; accepted 8 October 2009
DOI 10.1002/app.31584
Published online 17 December 2009 in Wiley InterScience (www.interscience.wiley.com).

ABSTRACT: PLLA-based eco-composites reinforced with kenaf fiber and rice straw and containing red or yellow pigments have been studied. The mechanical behavior of the composites was tested by DMTA at two different annealing temperatures (65°C and 85°C) and times (15 min and 120 min) as well as at two preparation conditions: vacuum drying and long time at room temperature. A decrease of microhardness was observed during the water absorption tests. Moreover, the rice straw-based composites absorbed more water than the kenaf-ones. Generally, the dyed NFs composites presented better water resistance than undyed ones. The pigments improved the adhesion and led to better mechanical performance. The natural fibers favored the cold crystallization process of PLLA and shifted the cold crystallization peak temperature to lower values, as it was confirmed by DSC measurements. The values of tensile storage modulus obtained after different preparation condition were strongly affected by the process of physical ageing. According to, tan δ parameter, the samples stored at room temperature for a long time showed the highest amorphous content. The PLLA eco-composite reinforced with kenaf fibers, dyed with the red pigment, and annealed at 85°C for 2 h displays the best mechanical properties. © 2009 Wiley Periodicals, Inc. J Appl Polym Sci 116: 1088–1098, 2010

Key words: poly(L-lactic acid); composites; fibers; ageing; annealing

INTRODUCTION

Many investigations in the recent years are referred to new materials with low price and good mechanical properties applied in different fields of social life. Ecologically friendly composites consist of a biodegradable matrix and different types of natural fibers (NFs), which have been successfully used long ago for reinforcing of polymer matrix. Quite recently, poly(lactic acid) (PLA) was used as a matrix for biodegradable eco-composites.[1–6] PLA is produced from renewable agricultural sources such as corn, and owns good stiffness and strength. Its L-enantiomeric form (PLLA) is known to exhibit better mechanical properties comparing with poly(D,L-lactic) acid.[7]

The low-crystallization rate of PLLA[8] allows its easy processing and, therefore, when searching for novel properties, PLLA is often modified with different monomers or reinforced with fibers. Usually, numerous nonwood lignocellulosic fibers, such as kenaf, jute, sisal, flax, hemp, or agricultural by-products, including stalks of most cereal crops, coconut, rice husks, peanut shells and other waste products, are used to create valuable properties of PLLA-reinforced materials. NFs, which are often used for reinforcing composites,[9–11] possess relatively high strength and stiffness, and their mechanical properties mainly depend on the cellulose content and the structure of the polymer: the fibril length and the microfibrilar angle.[12]

With relation to the advantages of NFs (low cost, recyclability, biodegradability), kenaf (*Hibiscus Cannabinus*) fibers can reduce carbon dioxide contamination in the atmosphere because the plant grows very fast, and rice (*Oryza sativa*) straw is an agricultural low-cost by-product. One of the most undesirable properties of NFs is their dimensional instability due to the swelling caused by moisture absorption. This

Correspondence to: T. Dobreva (tdobreva@clphchm.bas.bg).
Contract grant sponsor: EU FP6 program (INCO Project); contract grant number: INCO-CT-2004-509185.
Contract grant sponsor: MEC; contract grant numbers: Projects MAT 2005-00228 and MAT2007 65519-C02-01.
Contract grant sponsor: Secretaría de Estado de Universidades e Investigación del MEC; contract grant number: SB2005-0016.

phenomenon is mainly caused by the hydrogen bonding between water molecules and the hydroxyl groups present in the cellulose structure. However, a strong fiber/matrix interfacial adhesion can help to diminish the water penetration, reducing the hygroscopicity, and, consequently, avoiding the worsening of mechanical performances of composites.[13]

Dynamic mechanical thermal analysis (DMTA) is a useful technique for investigating the mechanical behavior of a material, regarding its viscoelasticity, and providing more information about a given polymer matrix than other mechanical tests because it covers a wide range of temperatures and frequencies. Three important parameters can be obtained during a dynamic mechanical test: (i) storage modulus, a measure of the maximum energy stored in the material during one cycle of oscillation, which gives an idea of the material stiffness; (ii) loss modulus, a parameter proportional to the amount of energy dissipated as heat by the sample; and (iii) loss tangent (tan δ), a mechanical damping term which is the ratio of the loss modulus to storage modulus and is related to the degree of molecular mobility in the polymeric material. Dynamic tests recorded over a wide range of temperature and at several frequencies are especially sensitive to all kinds of transitions and relaxation processes of matrix and interphase, to their activation energies, to adhesion of NFs and also to the morphology of the composites.

The tensile and flexural properties of PLLA as well as the spherulitic radius strongly depend on the molecular weight, thermal treatments applied to the polymer, and the processing techniques.[7,14–16] Also, the spherulites of PLA grow during the disorder-to-order phase transition, observed in the temperature range 100–120°C.[17] Moreover, many additives were investigated to improve the brittleness of raw PLLA, even though the flexibility increase of PLLA results in a decrease of crystallization temperature.[18] Another phenomenon taking place in PLLA is physical ageing, a reversible structural relaxation observed also with other composite systems, mainly when the glass temperature of the system is higher than room temperature.[19–21]

The dynamic mechanical properties of a composite material depend on the fiber length and distribution,[22] compatibilizer, interfacial bonding and also the mode of testing. One of the most important parameters obtained by DMTA is the glass transition temperature (T_g) defined as the maximum of the transition in the damping factor (tan δ) versus temperature curve. Usually, T_g is associated with a cooperative motion of long-chain polymer segments. In some polymers, a part of amorphous phase presents special properties which impose the appearance of a three phase model, with a rigid amorphous phase (RAF) which strongly depends on the thermal treatments and progressively disappears above T_g.[23,24] Jacob et al. have examined the dynamic mechanical behavior of sisal/oil palm hybrid fiber-reinforced natural rubber composites, and they observed a decrease of the damping factor, which indicated less content of amorphous phase.[25] Besides, when a poor interfacial adhesion for the PLA/poly(butylene succinate) blends exists, different peaks could be seen in the dynamic mechanical tests, associated with the glass transition of the each component.[26] However, the influence of different storage conditions on the mechanical properties of eco-composites has not been appropriately studied.

The aim of this work is to study the mechanical behavior of PLLA-based composites reinforced with kenaf fibers and rice straw, and the influence of physical ageing on the main mechanical properties and crystallization behavior, investigated by DMTA and DSC. The effect of annealing temperature as well as preparation conditions on those properties is also studied. Moreover, the water absorption affinity of eco-composites is analyzed and monitored by performing microhardness (MH) tests.

MATERIALS AND METHODS

Materials

Poly(L-lactic acid) (PLLA) (M_w = 118 kDa and density = 1.25 g/cm^3) was kindly supplied from Biomer (Krailling-Germany). Kenaf bast fibers, average length 5.1 mm and average diameter 21 μm, were received from Kenaf Eco Fibers Italia S.p.A. (Guastalla-Italy). The waste rice straw, average diameter less than 2 mm, was kindly supplied by the Rice Institute of Kocani, Macedonia. Pigments, Lysopac yellow 7010*N* (diazo-based substance, used for paints) and Lysopac red 7030 C (iron oxide used for plastics) were obtained from Cappelle, Belgium, and both have high light stability and good heat resistance.

Composites processing

Composites of PLLA and NFs were prepared by melt mixing in a Rheocord EC apparatus of Haake, NJ. The two kinds of composites were prepared by the following procedures: 37.5 g PLLA and 2.5 g proper coupling agent (CA) synthesized from maleic anhydride and dibenzoylperoxide were mixed in the Rheocord apparatus for 7 min at 175°C. The compatibilizing effect of this coupling agent was demonstrated in the previous published data by Avella et al.[6] Thereafter, 10 g of vacuum dried (for 24 h) kenaf fibers (rice straw) were added and the mixture was blended at 180°C for further 10 min, increasing progressively the mixing rate up to 32 rpm. Eventually, pigments and fire retardant (aluminum hydroxide) were also added to this mixture, and the same blending procedure was used.

TABLE I
Contents (% wt) of the Two Types of Lignocellulosic Natural Fibers, According to Ref. [10], and Length of the Kenaf and Rice Straw Fibers

NFs	Celulose (%)	Lignin (%)	Ash (%)	Silica (%)	Length (mm)
Kenaf fibers (KF) Blast fibers	44–57	15–19	2–5	0	5.1
Rice straw (RS) Straw fibers	28–48	12–16	15–20	9–14	2

Sheet specimens with thicknesses about 3.8 mm

Finally, the materials were compression molded at 180°C for 5 min, to obtain 80 × 10 × 3.8 mm^3 specimens. An average molecular weight of 61 kDa was determined for PLLA sheet specimen, by intrinsic viscosity measuremnet in chloroform at 25°C and used as a control test in our experiments.

Film specimens with thicknesses about 300 μm

The films were prepared using the aforementioned sheets at the following conditions: pressing at 190°C, 15 bar for 2 min, and after that, cooling for 3 min. An average molecular weight of 56 kDa for PLLA film specimen was determined. This value corresponded well with published data for the loss of molecular weight during the compression molding process.[14] The final composition of NFs composites is PLLA/CA/NFs = 75/5/20 wt %, and the corresponding samples are coded as PLLA-KF (kenaf fibers) and PLLA-RS (rice straw). For the dyed samples, the content of the dye is 4 wt % (PLLA/NF/dye = 66/17/4 wt %) and the corresponding codes are PLLA-KF-red and PLLA-RS-yellow. These dyed samples include also 8 wt % of a fire retardant, FR (the investigation about the fire retardance is outside the scope of the present work). The main characteristics of the NFs can be seen in Table I, whereas Table II lists the relative contents in the different samples.

Methods

Viscometric measurements

The molecular weight of poly(L-lactic) acid was measured viscometrically in a Ubbelohde-type viscometer in chloroform at 25°C. The viscosity molecular weight, M_v, was calculated from the intrinsic viscosity by using the following relation[27]:

$$[\eta] = 5.45 \times 10^{-4} M_v^{0.73} \quad (1)$$

Water absorption

Samples with dimensions 25 × 25 × 0.3 mm^3 were cut from film specimens and used to examine the water absorption behavior after vacuum drying at room temperature for 24 h. The samples were immersed in distilled water (25°C) for 72 h and taken out of the water at each 24 h. The percentage of water absorption (PWA) was calculated by the expression:

$$\mathrm{PWA} = \frac{(W_f - W_i)}{W_i} \times 100 \quad (2)$$

where W_f and W_i are the final and initial weights, respectively.

Dynamic mechanical thermal analysis

The sheet specimens with dimensions 25 × 10 × 3.8 mm^3 were analyzed in a Rheometrics DMTA V apparatus in the bending mode. The test-specimens were clamped on a dual-cantilever geometry. The temperature used in the experiments ranged from 25 to 160°C, at a heating rate of 1.5°C/min. The frequencies used were 1, 3, 10, and 30 Hz.

For the film specimens, the storage (E') and loss (E'') moduli and the loss factor (tan δ) were measured as a function of temperature (10–125°C) by using a Polymer Laboratories MK II dynamic mechanical thermal analyzer working in the tensile mode. Measurements were provided at four frequencies (1, 3, 10, and 30 Hz) at a constant heating rate of 1.5°C/min.

Thermal analyses

The differential scanning calorimetry (DSC) experiments were conducted in sealed aluminum pans using samples that weighted 8 ± 1 mg. All the

TABLE II
Composition of the Investigated Samples

PLLA	KF	RS	CA	Pigment	FR	Acronym
100						PLLA
75	20		5			PLLA-KF
75		20	5			PLLA-RS
66	17		5	4	8	PLLA-KF-red
66		17	5	4	8	PLLA-RS-yellow

All numbers are contents in % wt.

experiments were conducted under nitrogen atmosphere (flow rate 50 mL/min) using a TA Q100 instrument. The apparatus was calibrated on a regular basis using indium. A separate pan was used for each experiment to minimize the thermal degradation of PLLA. All samples were heated from −45 to 190°C at a heating rate of 1.5°C/min. The degree of crystallinity was calculated according to the following equation:

$$X_c = \frac{\Delta H_m}{\Delta H_m^0} \quad (3)$$

where ΔH_m is the neat enthalpy of melting, by integrating the DSC curve from around 65 to 180°C. The used ΔH_m^0 value for 100% crystalline PLLA is 91 J/g.[28] The DSC glass transition temperature (T_g) was taken as the temperature at the midpoint (1/2 Δc_p) of the transition. The melting temperature (T_m) was reported as the peak value of the melting endotherms. The cold peak crystallization temperatures obtained from DSC curves were reported as T_c^I and T_c^{II}.

The thermogravimetric analysis (TGA) was carried out with a Q500 Thermal Analysis Instrument, under nitrogen gas flow (20 mL/min) and with a heating rate of 10°C/min.

Microhardness

The microhardness (MHV) was determined by the Vickers method, where the indentor is a regular square-based diamond pyramid with top angle of 136°, applying the following equation:

$$\mathrm{MHV} = 2\sin 68^\circ P/d^2 \quad (4)$$

where d is the projected diagonal length of the imprint after releasing the indentor and $P = 0.981$ N is the applied load during a contact time of 25 s at room temperature. All measurements were performed according the standard methods, and thus, the values presented of the composite's properties represent the average value of 5 measurements.

Wide-angle X-ray diffraction (WAXD)

WAXD patterns were recorded in the reflection mode, at room temperature, by using a Bruker D8 Advance diffractometer provided with a Goebel mirror and a PSD Vantec detector (from Bruker, Madison, Wisconsin). Cu Kα radiation was used. The equipment was calibrated with different standards. A step scanning mode was used for the detector, with a 2θ step of 0.024° and 0.2 s per step.

RESULTS AND DISCUSSION

PLLA is a natural polymer with a glass transition around 60°C, well above room temperature; therefore, the polymer tends to go to the thermodynamic equilibrium when stored at RT and, its properties change along time and temperature. This behavior should be similar in the case of eco-composites based on PLLA as a matrix. To understand the final properties of PLLA composites, we have planned the experiments with control of the aforementioned parameters, time and temperature. The possible interactions between the PLLA matrix and different types of NFs were tested both by DMTA and DSC methods. Moreover, the water absorption of eco-composites has been also studied because of the hygroscopic nature of their structure.

Bending storage modulus for the sheet specimens annealed at 65°C and 85°C

A clear understanding of the storage modulus–temperature curves obtained during a dynamic mechanical test provides valuable insight into the stiffness of a material. Also, these curves, as well as the tan δ versus temperature one, are very sensitive to structural changes such as molecular weight and fiber–matrix interfacial bonding. The glass transition of PLLA-based composites was around 58°C i.e., far from the thermodynamic equilibrium when stored at RT, and that is why their properties could be affected by ageing. The physical ageing is a thermoreversible phenomenon characterizing the amorphous polymers below T_g so that when a sample is kept a definite time at a temperature above T_g this phenomenon disappears. Therefore, to avoid the possible ageing, we have treated the sheet specimens in an oven for 15 min at 65°C. Immediately after that we carried out DMTA and DSC measurements. The temperature of 65°C was chosen to be about 10°C above T_g. The obtained storage moduli for the composite materials are shown in Figure 1. It must be pointed out that the values presented in Figure 1(a) and Table III are without ageing influence, as ageing processes are not observed by DSC measurements [Fig. 1(b)]. Moreover, this thermal treatment does not produce any crystallinity, and these samples are initially totally amorphous (see below). The two types of NFs lead to an increase of the storage modulus of PLLA matrix because of the reinforced effect of lignocellulosic fibers. The composites with kenaf fibers displayed higher modulus than the rice straw ones. Moreover, the dyed composites presented better modulus than the undyed ones.

The cold crystallization phenomenon can be detected by DMTA and DSC tests. From Figure 1(a), it can be seen a second plateau region starting from

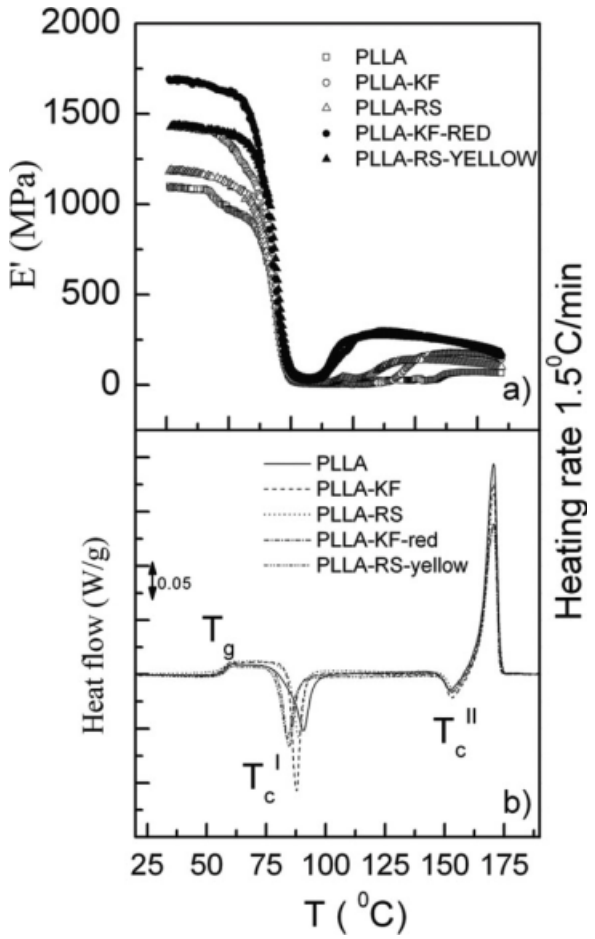

Figure 1 (a) DMTA scans recorded at 3 Hz and (b) DSC scans, both recorded after 15 min at 65°C, at the heating rate of 1.5°C/min.

different temperatures due to the cold crystallization. From Table III and Figure 1(b) (DSC results), we can say that the lignocellulosic fibers favored the cold crystallization because the first cold crystallization peak (T_c^I) shifted to lower temperatures. The NFs in the composites have obviously an influence only upon the first cold crystallization peak (T_c^I), decreasing the peak temperature for about 3–7°C. At the same time, the second cold crystallization peak (T_c^{II}), which corresponds with recrystallization of the melt unstable formed crystals, and melting temperatures (T_m) remained without change (Table III). The dyed samples presented a higher decrease of T_c^I comparing with undyed specimens, probably as consequence of possible nucleating effects of the dyes. Anyway, the neat enthalpy of melting from around 65 to 180°C is negligible for all samples, indicating that the initial degree of crystallinity is zero. This fact will be confirmed below by the X-ray diffraction experiments.

Analyzing the results of DMTA, it can be observed that at temperatures higher than T_g, the values of storage modulus are very low and practically the same for all eco-composites, but with increasing temperature and reaching the region of the cold crystallization, the moduli are increasing again. Although this behavior is not usual, it has been previously observed in metallocenic syndiotactic polypropylene, as a result of cold crystallization.[29]

It can be also seen in Figure 1(a) that all the samples display a similar drop during T_g, although the modulus decrease started at different temperatures. Thus, the T_g values were slightly lower for the composites than for PLLA-matrix, determined by both methods (DMTA and DSC). The parameters obtained from both methods are listed in Table III.

To study the influence of a higher temperature and prolonged time, the sheet specimens were treated in an oven at 85°C for 120 min. This second temperature (85°C) was chosen as close enough to the cold crystallization temperature of PLLA so that crystallization is attained. The obtained DMTA and DSC results after this treatment are presented in Figure 2. The storage modulus for the kenaf-dyed composite was again the highest, partly, due to the higher crystallinity in this sample (see Table IV). At the same time, the modulus of PLLA-KF composite is considerably lower (Table IV), probably, due to the worse interfacial bonding between crystallized matrix and kenaf fibers. Thus, the additional effect of the red dye is clearly deduced: the interfacial bonding between the matrix and the fibers has probably improved, and the modulus of this composite drastically changed compared with the others. This effect, however, is not observed in the RS composites, probably, due to the distinct characteristics of

TABLE III
Parameters Obtained from DMTA and DSC for the Sheet Specimens, Annealed at 65°C for 15 min

Samples	DMTA 65			DSC 65				
	E' at RT (MPa)	T_g (tan δ) (°C)	Tan δ intensity	T_g (°C)	T_c^I (°C)	T_c^{II} (°C)	T_m (°C)	X_c (%)
PLLA	1100 ± 50	76 ± 1	1.9	58	91	152	170.5	0
PLLA-KF	1440 ± 50	75	1.5	58	88	153	170.5	0
PLLA-RS	1190 ± 50	75	1.3	57	89	153	170.6	0
PLLA-KF-red	1700 ± 50	74	1.3	57	85	153	170.6	0
PLLA-RS-yellow	1420 ± 50	75	1.1	58	84	153	170.4	0

The estimated errors are E': ±50 MPa; Temperatures: ±1°C; tan δ: ±0.1.

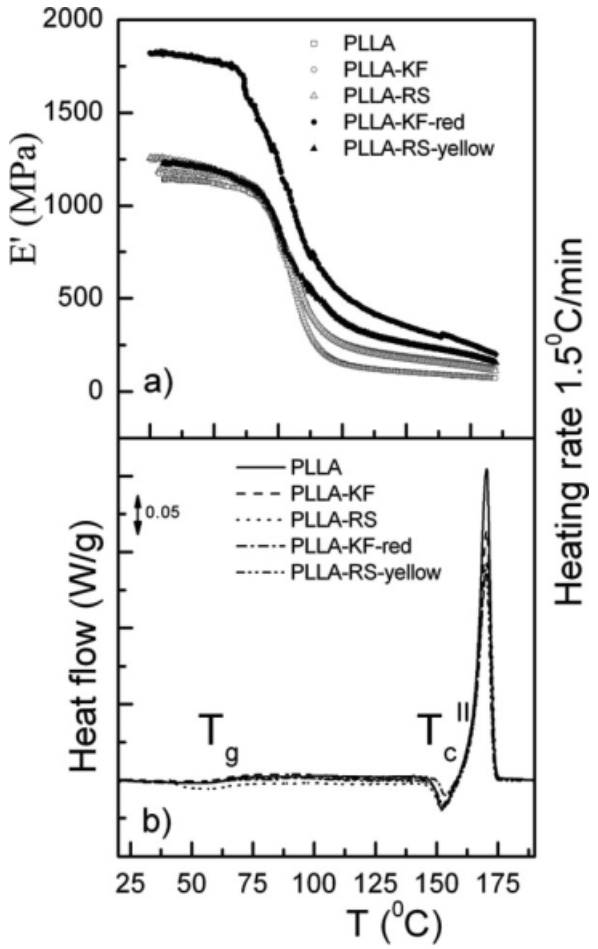

Figure 2 (a) DMTA scans recorded at 3 Hz and (b) DSC, both recorded after 120 min at 85°C, at the heating rate of 1.5°C/min.

the rice straw fiber (Table I). Moreover, the crystallinity of the PLLA-RS-yellow sample is considerably smaller than that for PLLA-KF-red.

Observing Figure 2(b), we can see that the cold crystallization disappeared, and calculating the crystallinity, we obtain the values for X_c as presented in Table IV. Moreover, comparing T_g65 and T_g85, we conclude that glass transition shifts toward higher temperatures after the annealing process performed at 85°C, as now all the samples display a considerable crystallinity.

The damping parameter (tan δ) is an important magnitude related to the analysis of the viscoelastic behavior of fiber reinforced composite structures. The major contribution to composite damping can be due to several factors: the nature of matrix, fibers, or interface; frictional damping due to slip in the unbound region between fiber and matrix interface (delaminations); damping as a result of energy dissipation in the matrix area; cracks and broken fibers. Thus, tan δ is related to the impact resistance of the material. The damping peak occurs in the region of the glass transition, where the material presents chain motions. Therefore, higher intensities of tan δ peaks were associated with the higher chain mobility, and tan δ peak intensity is usually related to the content of amorphous phase. According to the DSC melting enthalpy for specimens annealed at 65°C, the composites present insignificant crystallinities (Table III), whereas for those annealed at 85°C, the composites were crystallized, and the PLLA-KF-red composite displays the highest degree of crystallinity, 54% (see Table IV).

Consequently, the intensity of tan δ for the samples annealed at 65°C presented high values, similar to those of the amorphous polymer, and the activation energy values were higher than 400 kJ/mol, as usual for the main relaxation associated with the glass transition. The neat PLLA has the highest tan δ value indicating a large degree of mobility and, hence, good damping characteristics. The incorporation of fibers decreases the damping characteristics of composites as the fibers improve the crystallizability of PLLA matrix.

When the composites were annealed at 85°C, they crystallized and tan δ intensities are drastically diminished compared with those of the composites annealed at 65°C (Fig. 3). The crystals reduce the mobility of the amorphous phase, acting as entanglements.

Water absorption of the film specimens

All lignocellulosic fibers are characterized by polarity and affinity to absorb moisture. The amount of absorbed moisture depends on the chemical content

TABLE IV
Parameters Obtained from DMTA and DSC for the Sheet Specimens, Annealed at 85°C for 120 min

Samples	DMTA 85			DSC 85			
	E' at RT (MPa)	T_g (tan δ) (°C)	tan δ intensity	T_g (°C)	T_c^{II} (°C)	T_m (°C)	X_c (%)
PLLA	1130	85	0.3	64	152	170.3	43
PLLA-KF	1180	84	0.2	64	152	170.5	50
PLLA-RS	1260	83	0.2	64	152	170.5	42
PLLA-KF-red	1810	82	0.2	62	153	170.5	54
PLLA-RS-yellow	1230	82	0.2	65	153	170.2	44

The estimated errors are E': ±50 MPa; Temperatures: ±1°C; tan δ: ±0.1; X_c: ±5%.

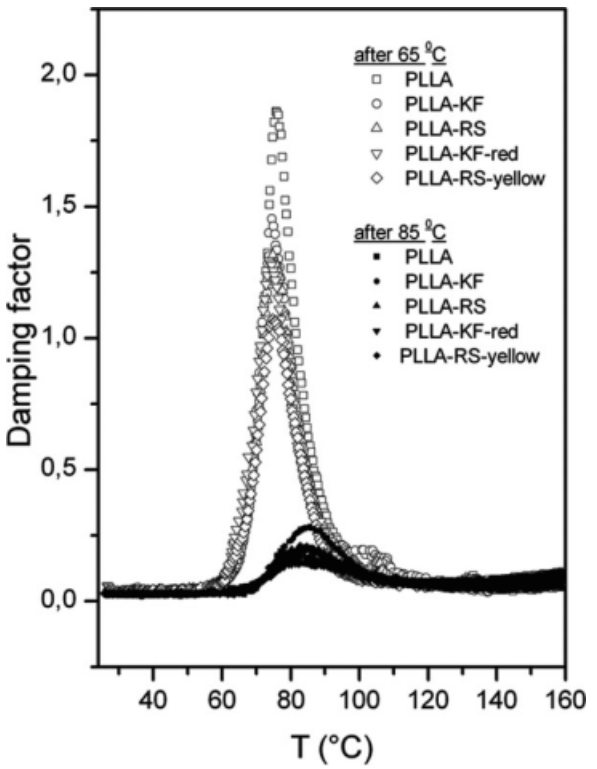

Figure 3 Results of tan δ for all composites at the two annealing temperatures.

and structure of the fibers. It is considered that fibers with higher lignin content show lower modulus and higher affinity to moisture absorbance.[30,31] But at the same time, the fibers with more lignin content present a better distribution in polymer matrix[32] and a better dyeing. To study the water absorbtion of PLLA-kenaf and rice straw composites, we used the film-type specimens.

The results of water absorption tests determined from immersion times of 24, 48, and 72 h were also controlled by MH measurements, as the absorbed water will have a certain influence on the final mechanical properties (in fact, MHV values can be directly related to the elastic modulus of the material[33,34]). The results in Figure 4 indicate that, as expected, the homopolymer PLLA showed the lowest water absorption. A published study reported that PLLA MH decreased significantly (≈ 60%) after 30 days immersion in a simulated body fluid solution at 37.5°C,[35] but other investigation showed an increase of MH about 55% during the storage at 37°C in a 15 days period due to the physical ageing.[36]

The MHV values [Fig. 4(b)] for 0 h were measured immediately after preparing the film specimens, just before their immersion in water. The PLLA-KF-red composite showed the highest value of MHV, besides its lowest water absorption after 24 h. As expected, a decrease of MH was observed after the water absorption tests. The lowest MHV values were obtained after performing 72 h-absorption test because the lignocellulosic polar fibers displayed a higher tendency to absorb water than the hydrophobic PLLA. Moreover, the rice straw fibers absorbed more water than kenaf fibers, and these results are in good accordance with the published data showing that the increase in lignin content leads to increased water absorption.[9,12] Even though we are referring to different composite materials, a study of polypropylene/rice straw composites (PP-RS = 50-50) showed that the percent of water absorbtion (PWA) was 3.8%,[31] and this value was comparable to PWA = 3.3% for PLLA-CA-RS = 75-5-20 composite. It could be concluded that the two used dyes have reduced the water absorbance capability of the composites, probably as a result of the established hydrogen bonds and by achieving better interfacial adhesion. Moreover, the kenaf dyed composite showed better water resistance than the rice straw dyed composite. A possible reason of this behavior could be the higher quantity of cellulose in kenaf fibers or the better interfacial bonding between matrix, fibers and dye, proving the consideration that less content of lignin leads to lower water absorbance. The MH test was used to examine the mechanical behavior in wet condition, and the obtained values are in good accordance with the water absorbance results. MHV of pure PLLA has showed even higher values after water absorbance, whereas

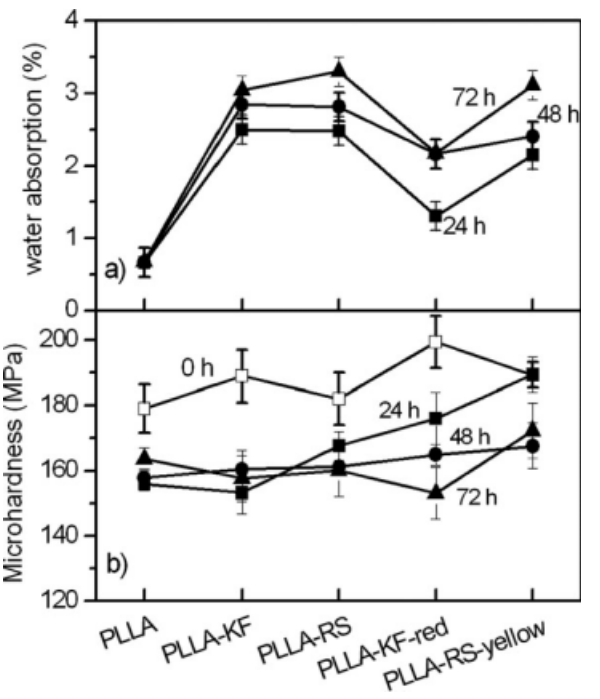

Figure 4 Results of (a) water absorption tests and (b) microhardness (MH) measurements after 0, 24, 48, and 72 h water immersion.

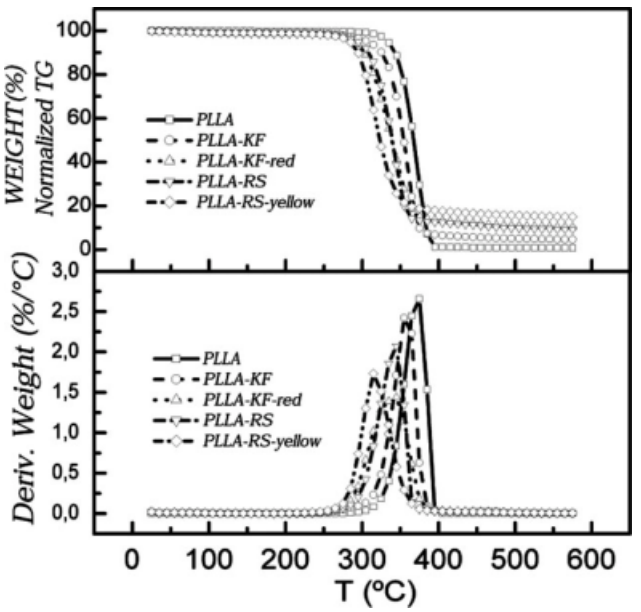

Figure 5 TGA curves (upper frame), registered at 10°C/min under nitrogen flow, and derivatives (lower frame) for the different samples.

the PLLA-RS composite absorbed more water than the other samples.

Thermal pyrolisis of waste plastics is drawing considerable attention not only on the perspective of solid waste management but also as an alternative source of energy or chemical raw materials. With these considerations, we have performed a thermogravimetric analysis of the samples. The corresponding TGA curves are shown in Figure 5. It can be observed that PLLA is a thermally very sensitive polymer and its degradation starts somewhat above 200°C, progressing until complete mass loss. The temperature for 50% weight loss is 367°C, and the derivative of the weight loss (lower part of Fig. 5) presents a maximum centered at 370°C.

The thermal degradation of PLLA has been reported to be a one-step process, with a first order kinetics.[37] The mechanism of thermal degradation is based upon a hydroxyl-end initiated process, leading to cyclic oligomers, lactide, acetaldehyde, and carbon monoxide as final products.[38,39] Regarding the composites, it can be observed in Figure 5 that the degradation of all of them is produced at lower temperatures than in the case of pure PLLA. Thus, the maximum in the derivative appears at a temperature 11°C lower for PLLA-KF. The difference is around 30°C for PLLA-KF-red and PLLA-RS, and the maximum difference, 53°C, is found for PLLA-RS-yellow. Therefore, the fact that the composites degrade at lower temperature than PLLA represents another interesting feature of these materials. On the other hand, TGA curves after 72 h immersion in water (not included) present a decrease in the degradation temperature of about 10°C comparing with the samples without water immersion.

Tensile storage modulus for vacuum dried films

After preparing the film specimens, some of them were stored at room temperature for ~ 1 month (undried films), and others were dried in a vacuum dessicator for 48 h at room temperature (dried films). The DMTA analysis was carried out using tensile mode, to compare the results of the film-type specimens under the aforementioned different preparation conditions. Immediately after that the dynamic mechanical tests in tensile mode (DMTA II) were carried out, the storage modulus, T_g and tan δ were measured and compared (see Table V).

By comparing the values obtained for the storage modulus at different preparation conditions, undried and dried films, it can be observed that the undried PLLA film increased its storage modulus and presented the highest modulus compared with the composite materials (Fig. 6). Therefore, the vacuum drying had a negative influence upon the modulus of PLLA i.e., the value is slightly lower than the undried film. Also, the dried composite PLLA-KF showed lower modulus than the undried one. Indeed, only an improvement of tensile modulus for PLLA-KF-red dry composite may be observed, possibly due to the better adhesion between fiber, matrix, and dye. At the same time, the dry conditions

TABLE V
Parameters from DMTA for Dried and Undried Films, and DSC for Undried Films. T_g Values from DSC of Undried Films Cannot be Correctly Determined due to the Physical Ageing (see Figure 9)

	DMTA undried films			DMTA dried films			DSC undried films		
Samples	E' at 24°C (MPa)	T_g (°C)	Tan δ intensity	E'at 24°C (MPa)	T_g (°C)	Tan δ intensity	X_c (%)	T_g (°C)	T_c^I (°C)
PLLA	3380	66	2.4	3100	66	2.1	0	55	92
PLLA-KF	2870	66	1.5	2500	66	1.2	0	54	88
PLLA-RS	2300	65	2.2	2550	66	1.6	0	54	89
PLLA-KF-red	3100	66	1.4	4300	65	0.9	0	54	86
PLLA-RS-yellow	2600	66	1.7	2400	66	1.0	0	53	84

The estimated errors are E': ±50 MPa; Temperatures: ±1°C; tan δ: ±0.1.

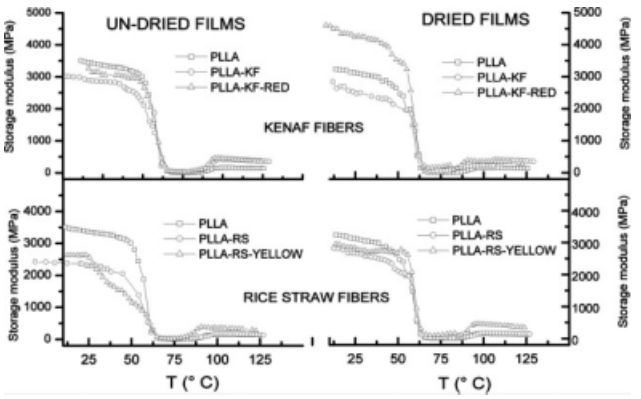

Figure 6 Storage modulus versus temperatures for the film specimens stored in different conditions: undried films—30 days at room temperature, dried films—several days in a vacuum dessicator.

slightly improved the tensile modulus of RS composites.

It must be stressed that the specimens stored during 1 month at RT present two competitive effects: the possible increase of modulus due to the ageing process and the decrease due to the water absorption. The final result is the similarity of the modulus values of those specimens when comparing them with the dried films.

According to the DSC scans, the undried film specimens crystallized during the heating and two cold crystallization peaks can be observed (Fig. 7), similarly to the sheet specimens annealed at 65°C for 15 min [Fig. 1(b)]. The cold crystallization peak temperatures (T_c^I) of undried films are presented in Table V. Comparing with T_c^I of sheet specimens annealed at 65°C (Table III), we can conclude that the peak temperature (T_c^I) appeared at the same

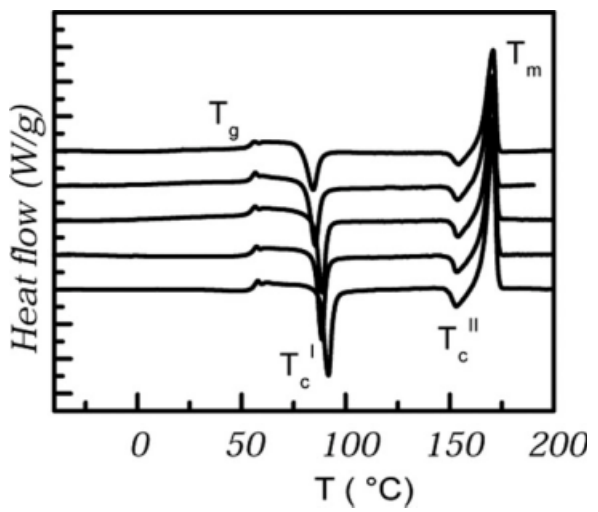

Figure 7 DSC scans recorded during the heating at 1.5°C/min for the undried films (from bottom to top, as following PLLA, PLLA-KF, PLLA-RS, PLLA-KF-red and PLLA-RS-yellow).

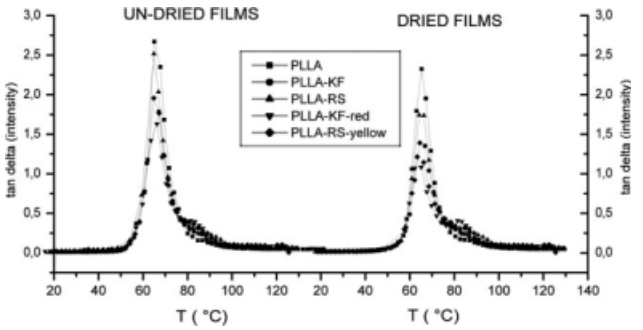

Figure 8 Results of tan δ intensities for undried and dried film specimens. Both types of specimens are initially amorphous.

location. These temperatures have not been influenced upon the different thermal conditions (15 min at 65°C and 1 month at RT).

The T_g values determined from tan δ maximum do not change very much and the values are comparable with the DSC ones. Also, the shapes of tan δ peaks are almost symmetrical (Fig. 8). The degree of crystallinity calculated from the peaks of Figure 1(b) and Figure 7 is negligible for all the samples. Moreover, both undried and dried composites displayed a lower value for T_c^I than PLLA matrix due to the nucleating effect of lignocellulosic fibers.

But observing the tan δ intensity, we may conclude that the vacuum dried films exhibit a smaller intensity comparing with undried (stored 1 month at room temperature) films (Table V and Fig. 8). The data from Figure 8 could be also associated with the ageing process, proved by the DSC results (Fig. 9).

Thus, the main difference between the two kinds of investigated specimens was the physical ageing, clearly seen in the specimens stored 1 month at RT. It is also possible a change in the amount of RAF during the thermal treatments, which lead to the different reported mechanical performance.[23,24] The RAF decreases and progressively disappears at temperature above T_g, since 15 min at 65°C is sufficient to eliminate both the RAF and the ageing process. It seems, therefore, that the tensile modulus for undried films is strongly influenced by ageing.

Using tan δ intensity as a measure of content of amorphous phase (this parameter was not affected by the sample geometry for the two types of DMTA tests), we can say that the different thermal treatments have influence over the quantity of amorphous phase (Fig. 10). Obviously, the samples annealed at 85°C present the lowest content of amorphous phase, and the values of the fall of storage modulus can be associated with the crystallinity (X_c) calculated by DSC scans by eq. (3) and listed in Table IV. The other thermal process (15 min at 65°C) only eliminated the physical ageing, but the samples remained amorphous. For the dried and undried

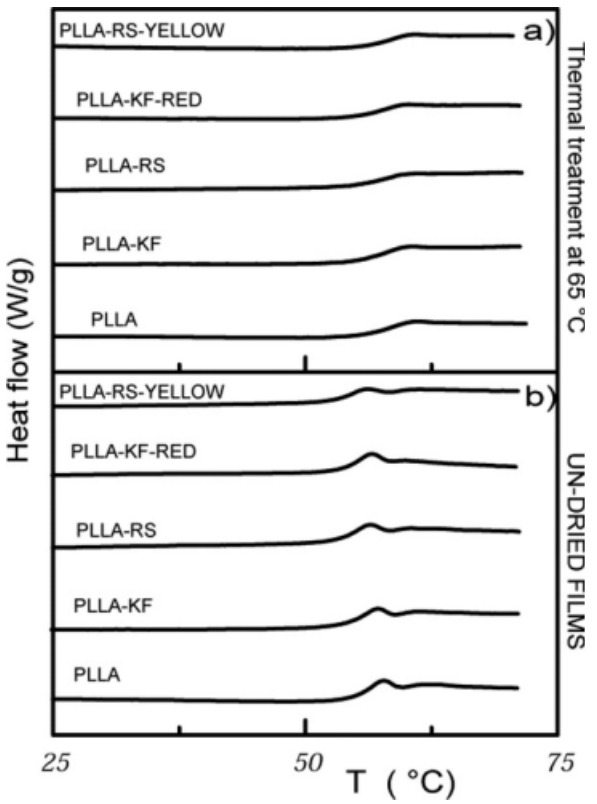

Figure 9 Glass transitions and physical ageing for two thermal treatments: (a) 15 min at 65°C (T_g without ageing), and (b) undried films, stored 30 days at RT (a clear ageing process is observed).

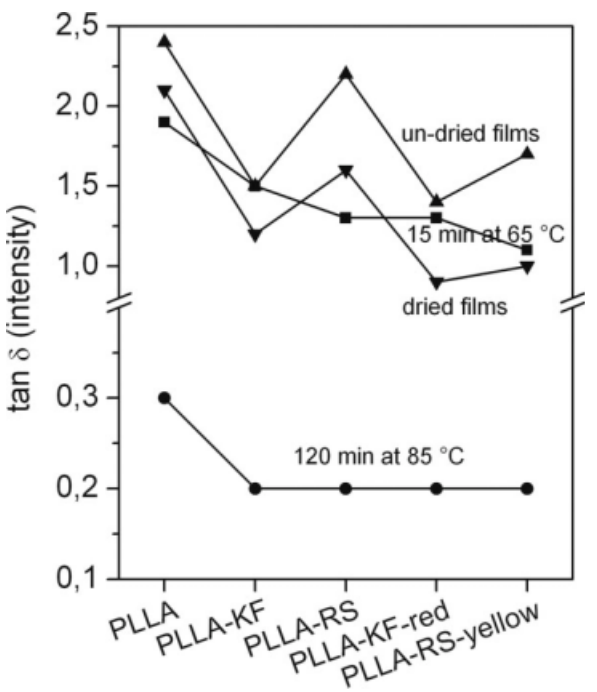

Figure 10 Data of tan δ intensities for all kinds of thermal treatments in the different composites.

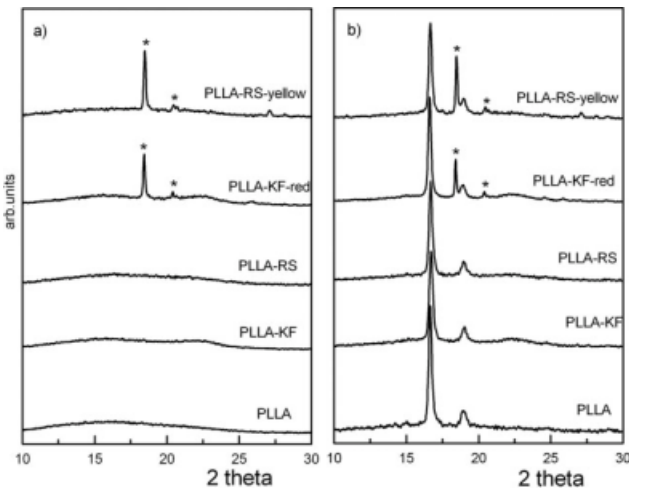

Figure 11 WAXD diffractograms recorded at room temperature; (a) after 15 min annealing at 65°C; (b) after 120 min annealing at 85°C. The asterisks indicate the peaks arising from the pigments.

films, tan δ follows the same trend for all the composites. However, it is clearly seen that the amorphous mobile content is smaller for dried films: the results of tan δ intensity for undried films were influenced by ageing, and, therefore, these values were higher than those of dried or annealed films. During the vacuum drying, the material underwent a supplement organization and the amorphous mobile content decreased for all composites.

Additional information about the effect of thermal treatment on the crystallinity of the samples was obtained from WAXD. The corresponding diffractograms are presented in Figure 11. It can be clearly observed that the PLLA component in all the specimens annealed at 65°C is completely amorphous, as the two main PLLA diffractions at around 16.6 and 19° are absent (only the peaks arising from the pigments are observed). On the contrary, those two crystalline diffractions from PLLA are clearly observed in all the specimens annealed at 85°C.

As a final aspect, the data from Tables III, IV, and V followed the same trend on T_g change by DMTA and DSC tests, even when T_g values determined by DMTA are higher than DSC ones, as usual.[40,41] Moreover, as pointed out earlier, the highest T_g values were displayed by the specimens annealed at 85°C for 2 h, where the samples were crystallized and the chain motions were hindered.

CONCLUSIONS

Studying the influence of different thermal treatments on PLLA eco-composites, we conclude that the one performed at 65°C (15 min) has resulted in removal of the effects of the physical ageing, but the

specimens remain amorphous. On the contrary, the treatment at 85°C (120 min) causes disappearance of the cold crystallization peak because of previous completion of crystallization, and as a result, the T_g values slightly increased.

The water absorption test indicates more water affinity of PLLA-RS composites than PLLA-KF ones. Moreover, the dyed specimens exhibited better mechanical properties in wet condition than the undyed ones.

Comparing the two different preparation conditions, it follows that the modulus of composites stored 1 month at room temperature was strongly influenced by ageing process and that during the vacuum drying, the amorphous phase underwent a supplement organization.

The PLLA-KF-red composite presents the highest storage modulus after each thermal treatment, as well as a higher degree of crystallinity after annealing at 85°C for 120 min.

In general, the NFs increase considerably the crystallization ability of PLLA, and the pigments lead to better mechanical properties.

References

1. Huda, M. S.; Mohanty, A. K.; Drzal, L. T.; Schut, E.; Misra, M. J Mater Sci 2005, 40, 4221.
2. Mathew, A. P.; Oksman, K.; Sain, M. J Appl Polym Sci 2005, 97, 2014.
3. Nishino, T.; Hirao, K.; Kotera, M.; Nakamae, K.; Inagaki, H. Compos Sci Technol 2003, 63, 1281.
4. Ke, T.; Sun, X. J Appl Polym Sci 2003, 89, 1203.
5. Oksman, K.; Skrifvars, M.; Selin, J. F. Compos Sci Technol 2003, 63, 1317.
6. Avella, M.; Bogoeva-Gaceva, G.; Bužarovska, A.; Errico, M. E.; Gentile, G.; Grozdanov, A. J Appl Polym Sci 2008, 108, 3542.
7. Perego, G.; Cella, G. D.; Bastioli, C. J Appl Polym Sci 1996, 59, 37.
8. Mano, J. F.; Wang, Y.; Viana, J. C.; Denchev, Z.; Oliveira, M. J. Macromol Mater Eng 2004, 289, 910.
9. Ndazi, B.; Tesha, J. V.; Bisanda, E. T. N. J Mater Sci 2006, 41, 6984.
10. Mohanty, A. K.; Misra, M.; Drzal, L. T. J Polym Environ 2002, 10, 19.
11. García, M.; Garmendia, I.; García, J. J Appl Polym Sci 2008, 107, 2994.
12. Bogoeva-Gaceva, G.; Avella, M.; Malinconico, M.; Buzarovska, A.; Grozdanov, A.; Gentille, G.; Errico, M. E. Polym Compos 2007, 28, 98.
13. George, J.; Sreekala, M. S.; Thomas, S. Polym Eng Sci 2001, 41, 1471.
14. Migliaresi, C.; Cohn, D.; De Lollis, A.; Fambri, L. J Appl Polym Sci 1991, 43, 83.
15. Tsuji, H.; Ikada, Y. Polymer 1995, 36, 2709.
16. Mohanty, A. K.; Wibowo, A.; Misra, M.; Drzal, L. T. Compos Part A 2004, 35, 363.
17. Zhang, J.; Tashiro, K.; Tsuji, H.; Domb, A. J. Macromolecules 2008, 41, 1352.
18. Martin, O.; Avérous, L. Polymer 2001, 42, 6209.
19. Pérez, E.; Pereña, J. M.; Benavente, R.; Bello, A.; Lorenzo, V. Polym Bull 1992, 29, 233.
20. Benavente, R.; Pereña, J. M.; Pérez, E.; Bello, A. Polymer 1994, 35, 3686.
21. Chung, H. J.; Yoo, B.; Lim, S. T. Starch 2005, 57, 354.
22. Shibata, S.; Fukumoto, I.; Cao, Y. Polym Compos 2006, 27, 170.
23. Arnoult, M.; Dargent, E.; Mano, J. F. Polymer 2007, 48, 1012.
24. Picciochi, R.; Wang, Y.; Alves, N. M.; Mano, J. F. Colloid Polym Sci 2007, 285, 575.
25. Jacob, M.; Francis, B.; Thomas, S.; Varughese, K. T. Polym Compos 2006, 27, 671.
26. Yokohara, T.; Yamaguchi, M. Europ Polym J 2008, 44, 677.
27. Schindler, A.; Harper, D. J Polym Sci 1979, 17, 2593.
28. Pyda, M.; Bopp, R. C.; Wunderlich, B. J Chem Thermodyn 2004, 36, 731.
29. Arranz-Andrés, J.; Benavente, R.; Ribeiro, M. R.; Pérez, E.; Cerrada, M. L. Macromol Chem Phys 2006, 207, 1564.
30. Reddy, N.; Salam, A.; Yang, Y. Macromol Mater Eng 2007, 292, 458.
31. Toro, P.; Quijada, R.; Murillo, O.; Yazdani-Pedram, M. Polym Int 2005, 54, 730.
32. Wang, Y.; Gómez Ribelles, J. L.; Salmerón Sánchez, M.; Mano, J. F. Macromolecules 2005, 38, 4712.
33. Zamfirova, G.; Lorenzo, V.; Benavente, R.; Pereña, J. M. J Appl Polym Sci 2003, 88, 1794.
34. Scrivani, T.; Benavente, R.; Pérez, E.; Pereña, J. M. Macromol Chem Phys 2001, 202, 2547.
35. Saiz-Arroyo, C.; Wang, Y.; Rodriguez-Perez, M. A.; Alves, N. M.; Mano, J. F. J Appl Polym Sci 2007, 105, 3858.
36. Wang, Y.; Mano, J. F. J Appl Polym Sci 2006, 100, 2628.
37. Gupta, M. C.; Deshmukh, V. Colloid Polym Sci 1982, 260, 514.
38. McNeill, I. C.; Leiper, H. A. Polym Degrad Stab 1985, 11, 267.
39. McNeill, I. C.; Leiper, H. A. Polym Degrad Stab 1985, 11, 309.
40. Cerrada, M. L.; Benavente, R.; Pérez, E.; Pereña, J. M. J Polym Sci Part B Polym Phys 2001, 39, 1.
41. Prieto, O.; Pereña, J. M.; Benavente, R.; Pérez, E.; Cerrada, M. L. J Polym Sci Part B Polym Phys 2003, 41, 1878.